Assessment of Macular Function for Idiopathic Epiretinal Membranes Classified by Spectral-Domain Optical Coherence Tomography

Jong-uk Hwang,[1] *Joonhong Sohn,*[2] *Byung Gil Moon,*[1] *Soo Geun Joe,*[1] *Joo Yong Lee,*[1] *June-Gone Kim,*[1] *and Young Hee Yoon*[1]

Purpose. To evaluate the functional changes in various morphologic types of idiopathic epiretinal membrane (ERM) by multifocal electroretinography (mfERG) and spectral-domain optical coherence tomography (SD-OCT).

Methods. All patients ($n = 71$) with unilateral idiopathic ERM underwent complete ophthalmologic examination, including measurements of best-corrected visual acuity (BCVA), SD-OCT, and mfERG for both eyes. To classify idiopathic ERM by subtype, the morphologic characteristics of the foveal area on representative scanned images were assessed. The five subtypes by foveal SD-OCT morphology included fovea-attached ERM with outer retinal thickening and minimal inner retinal change (Group 1A), outer retinal inward projection and inner retinal thickening (Group 1B), and prominent thickening of inner retinal layer (Group 1C) and foveal sparing ERM with formation of macular pseudohole (Group 2A) and with schisislike, intraretinal splitting (Group 2B).

Results. On mfERG, P1 amplitude density in the central ring (R1) and inter-eye (affected eye/fellow eye) response ratio of P1 amplitude density in R1 differed significantly among five groups ($P = 0.032$ and $P = 0.022$, respectively). In Group 1 patients, central subfield thickness (CST) and inner retinal layer thickness (IRT) on SD-OCT were strongly correlated with BCVA and P1 amplitude density in R1. A receiver operating characteristic (ROC) curve analysis showed that IRT had high predictive accuracy in distinguishing Groups 1A and 1B (area under the ROC curve [AUROC] = 0.966) and Groups 1B and 1C (AUROC = 1.000).

Conclusions. Multifocal electroretinography can be used to investigate the pathophysiology of ERM and to evaluate the degree of functional demise in the fovea on SD-OCT. (*Invest Ophthalmol Vis Sci.* 2012;53:3562–3569) DOI:10.1167/iovs.12-9762

From the [1]Department of Ophthalmology, Asan Medical Center, University of Ulsan College of Medicine, Seoul, Korea; and the [2]Division of Vitreoretinal Surgery, Hangil Eye Hospital, Incheon, Korea.

Presented at the 5th Congress of the Asia-Pacific Vitreo-Retinal Society, Singapore, November 2010.

Submitted for publication February 26, 2012; revised April 16, 2012; accepted April 16, 2012.

Disclosure: **J. Hwang**, None; **J. Sohn**, None; **B.G. Moon**, None; **S.G. Joe**, None; **J.Y. Lee**, None; **J.-G. Kim**, None; **Y.H. Yoon**, None

Corresponding author: Young Hee Yoon, Department of Ophthalmology, Asan Medical Center, University of Ulsan College of Medicine, #388-1, Pungnap-Dong, Songpa-Gu, Seoul 138-736, Korea; yhyoon@amc.seoul.kr.

Surgery for idiopathic epiretinal membrane (ERM) has been a common vitreoretinal procedure for many years. The principal indication for ERM surgery is vision disturbance resulting from decreased visual acuity with or without metamorphopsia.[1] Despite approximately 70% to 80% of the patients who have undergone the operation experience a significant improvement of vision in the operated eye,[2,3] limited improvement of visual acuity may occur after successful ERM removal in the absence of significant complications.[4] This might be caused by the absence of well-defined classification of ERM. Previously reported classification systems were based on the clinical scale[5] or time-domain optical coherence tomographic findings,[6,7] but their structural classifications were not supported by relevant objective functional data. Accordingly, these classifications would not permit a better estimate of prognosis and relative urgency of ERM surgery.

Multifocal electroretinography (mfERG) is a noninvasive, objective method to detect regional functional changes in the central retina by measuring electrophysiologic responses.[8] This method has been shown useful in assessing macular function before and after surgery in eyes with ERM.[9,10] To date, however, mfERG has not been used in investigations of spectral-domain optical coherence tomography (SD-OCT) based morphologic classifications of ERM, despite the importance of objectively classifying graded functional compromise after chronological, structural derangement of the retina caused by ERM.[6,7] We therefore investigated the new classification system for idiopathic ERM by evaluating SD-OCT–based morphologic characteristics, and by functional assessment of the macula using mfERG.

Methods

Study Participants and Clinical Examinations

The study was a nonrandomized, retrospective consecutive case series, assessing preoperative data of patients who underwent surgery for idiopathic unilateral ERM, with all operations performed by one surgeon (YHY) in our institution. Patients with bilateral ERM were excluded, as were patients with other secondary causes of ERM, such as diabetic retinopathy, retinal vein occlusion, peripheral retinal tear, vitreomacular traction, and uveitis, all of which may have altered retinal physiology and mfERG responses. Because cataracts or intraocular lenses may cause large variations in mfERG response, we also excluded patients with visually significant cataracts, differences in cataract severity of both eyes, and pseudophakia. We also excluded eyes with reduced vision attributed to other retinal pathologies, such as glaucoma, as confirmed by glaucomatous optic nerve head changes and visual field tests, and age-related macular degeneration.

ERM was assessed by biomicroscopy and SD-OCT (Cirrus HD; Carl Zeiss Meditec, Dublin, CA). Best-corrected visual acuity (BCVA) was measured at the time of SD-OCT, using a logMAR-based vision chart (Jin's Vision Chart; JV Institute, Seongnam-City, Korea). Objective macular function was assessed using mfERG (RETI-scan version 3.2; Roland Consult Stasche & Finger GmbH, Brandenburg an der Havel, Germany). Informed consent was obtained from all subjects after we explained the recording procedures. This study conformed to the tenets of the Declaration of Helsinki.

Optical Coherence Tomography

The scan acquisition protocol for high-definition optical coherence tomography (Cirrus HD-OCT) was a macular cube 512 × 128 combo, consisting of 512 horizontal A-scans measured with 128 vertical lines across an area of 6 × 6 mm (sample densities of approximately 47 μm between A-scans in the superior–inferior direction and approximately 12 μm in the temporal–nasal direction). Scans with signal strength greater than 7/10 were considered appropriate, and a representative horizontal raster scan image passing the foveola was selected for each eye after thorough review of scan data by two retinal specialists (JH and YHY). To classify idiopathic ERM into its subtypes, we assessed the morphologic characteristics of the foveal area (1.5 mm length) in the representative scan image (Fig. 1). A topographic surface map was constructed for each eye using the automated software algorithms and displayed with numeric averages of the thickness for each of the nine map sectors defined by the Early Treatment Diabetic Retinopathy Study (ETDRS).[11] Final analysis was performed on scans after manually correcting for segmentation errors. Central subfield thickness (CST) was defined as the average thickness in the central 1-mm subfield centered at the fovea. Inner retinal layer thickness (IRT) was defined as the distance from the vitreoretinal interface to the inner border of the outer nuclear layer at the foveal center (Fig. 1). The IRT was calculated using our institution-based image analysis system. The outer retinal layer denoted layers of photoreceptor, encompassing the outer nuclear layer and inner segment/outer segment (IS/OS) junction line in OCT scan images.

Classification of Epiretinal Membranes

Patients with idiopathic ERM were classified into five groups based on their SD-OCT–determined morphologic characteristics in the foveal area. In general, patients were divided into two groups, depending on whether ERM involved the foveal area (Fig. 2). Group 1 included ERMs involving the fovea (fovea-attached type), and Group 2 included ERMs sparing the fovea (pseudohole type).

Fovea-attached ERM (Group 1) could be subdivided into three groups (Fig. 3). Group 1A included ERM with outer retinal thickening; the inner retina, however, showed a minimal increase in thickness and maintained a nearly normal configuration. Group 1B included ERM with more exaggerated tenting of the outer retinal layer in the foveal area; the inner retinal layer was slightly thickened and its configuration was distorted by centripetal and anteroposterior tractional forces due to ERM. Group 1C included ERM with prominent inner retinal thickening, with inward tenting of the outer retinal reflectivity in the foveal area. Pseudohole-type ERM (Group 2) could be divided into two groups (Fig. 3). Group 2A included ERM with the formation of a macular pseudohole, whereas Group 2B included ERM with macular pseudohole accompanied by marked intraretinal splitting.

mfERG

We recorded mfERG responses using a modified camera system (RETI-scan system; Roland Consult) after 10 minutes of light adaptation. The recording protocol followed the guidelines of the International Society for Clinical Electrophysiology of Vision (ISCEV).[12] Pupils were fully dilated with 1.0% tropicamide and 2.5% phenylephrine. The stimulus consisted of 103 hexagonal elements, covering 27° of the visual field, and presented on a 20-inch cathode ray tube monitor at a viewing distance of 30 cm. Stimulus monitor luminance settings were 100 cd/m^2 (white hexagonal elements) and 1.0 cd/m^2 (black hexagonal elements), which achieved a contrast of approximately 99%. Refractive errors were corrected for the viewing distance. To obtain a good signal-to-noise ratio, we used an ERG-jet electrode (Fabrinal SA, La Chaux-De-Fonds, Switzerland), with each individual's forehead serving as a ground. Target fixation during the recording was performed using a 5°-sized red cross at the center of the stimulus monitor. Fixation was checked by online video-monitoring during each recording session, which lasted up to 8 minutes. To improve fixation stability, sessions were broken into 47-second segments, with eight trials recorded during each session. Segments containing high-amplitude artifacts were discarded and repeated. Signals were amplified with a gain of 10^6, band-pass filtered (5–100 Hz), and recorded with a sampling frequency of 1020 Hz.

First-order kernels of mfERG were analyzed. Local responses were divided by the respective stimulus area to obtain the density-normalized response (nV/deg^2). For each hexagon, the N1 and P1 amplitudes were calculated. To evaluate retinal function in the foveal

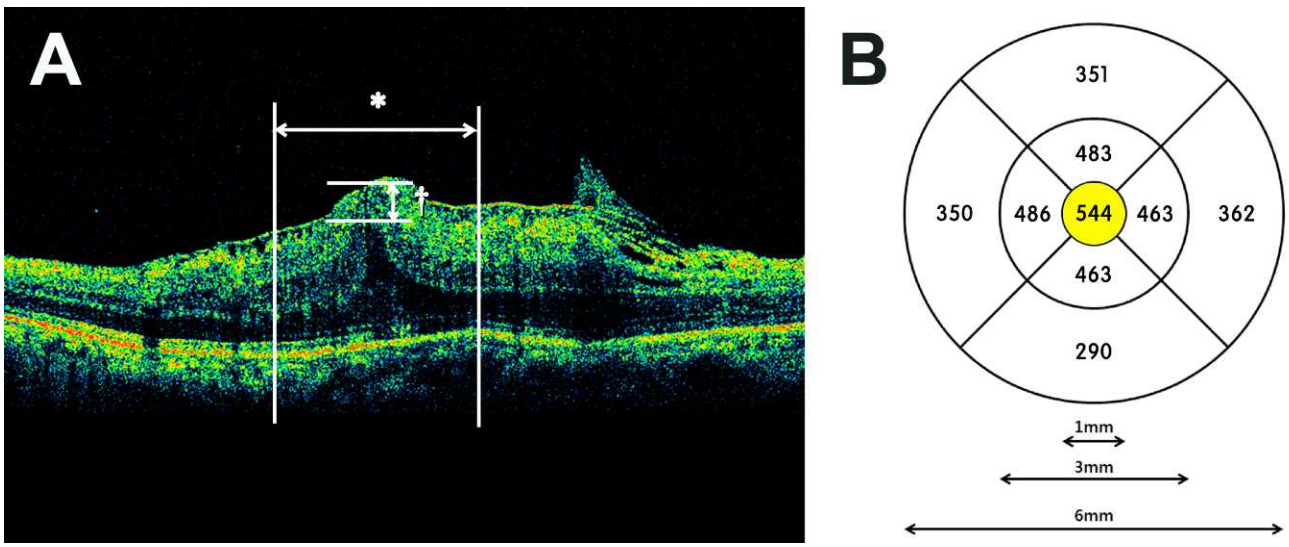

Figure 1. (**A**) Representative SD-OCT scan image showing the 1.5-mm foveal area investigated. (**B**) Numeric averages of the thicknesses of the nine map sectors, as defined by the Early Treatment Diabetic Retinopathy Study (ETDRS). The central subfield thickness (CST) represents the average thickness of the central 1 mm diameter ring (*yellow area*). *1.5 mm foveal area; †Inner retinal layer thickness (IRT).

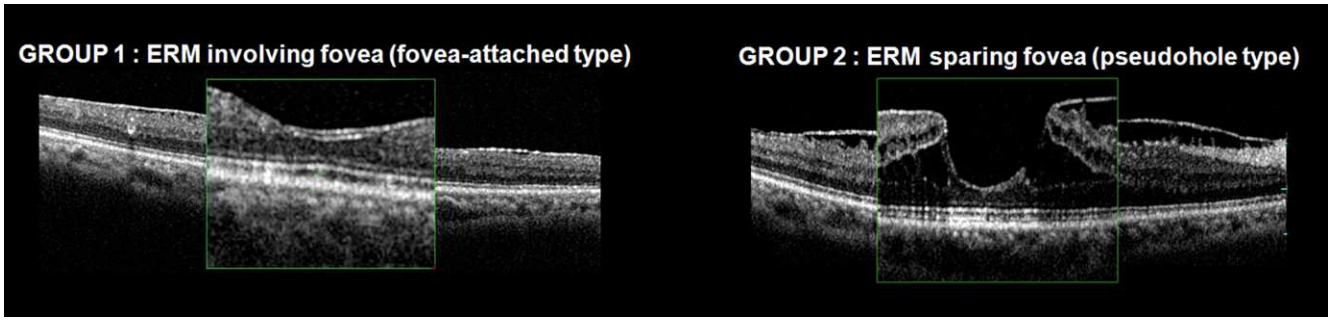

Figure 2. Representative SD-OCT images showing examples of fovea-attached (Group 1) and pseudohole type (Group 2) ERMs. No reflectivity consistent with ERM was observed in the foveal area of pseudohole-type ERM.

area corresponding to a central 1.5-mm area in the representative SD-OCT scan image, these amplitude parameters were analyzed in ring 1 (R1) and ring 2 (R2) of each group average map, which consisted of six concentric rings (Fig. 4).

Inter-Eye Response Ratio

Inter-eye response ratio for each participant was calculated as the response in the affected eye divided by the response in the unaffected eye, without retinal pathology. Thus, this ratio parameter can minimize individual variations in mfERG responses.

Statistical Analysis

Statistical comparisons were made using ANOVA tests and Pearson correlation factors. Receiver operating characteristic (ROC) curves were used to determine the overall predictive accuracy of the SD-OCT parameters, as described by the area under the ROC curve (AUROC), as

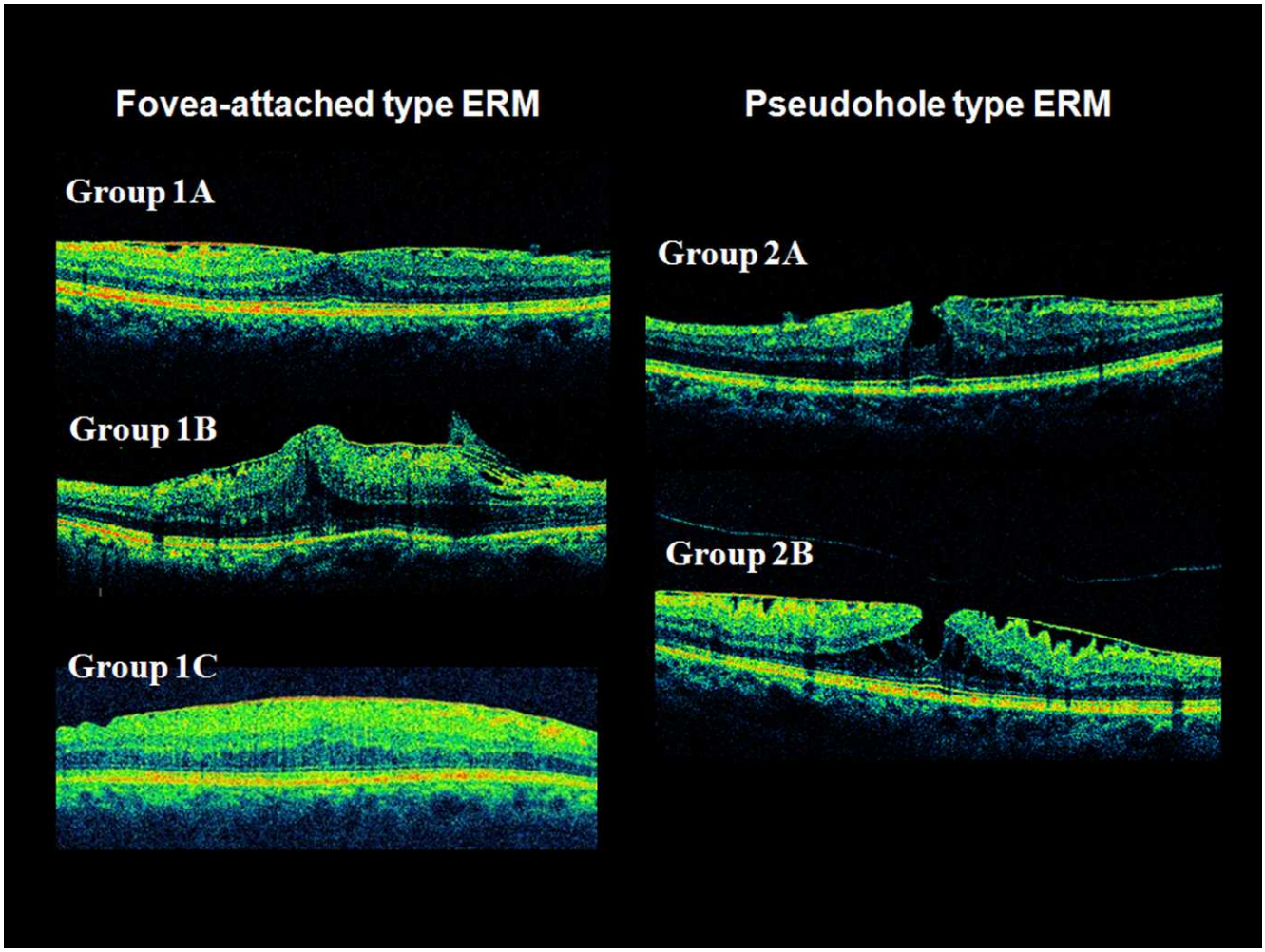

Figure 3. SD-OCT–based morphologic classification of idiopathic ERM. Group 1A, ERM with outer retinal thickening and near-normal inner retina. Group 1B, ERM with exaggerated tenting of the outer retinal layer in the foveal area; the inner retinal layer was slightly thickened and its configuration was distorted by centripetal and anteroposterior tractional forces caused by ERM. Group 1C, ERM with prominent inner retinal thickening; little inward tenting of outer retinal reflectivity was observed in the foveal area. Group 2A, ERM with formation of a macular pseudohole (MPH). Group 2B, ERM composed of MPH and accompanied by marked intraretinal splitting.

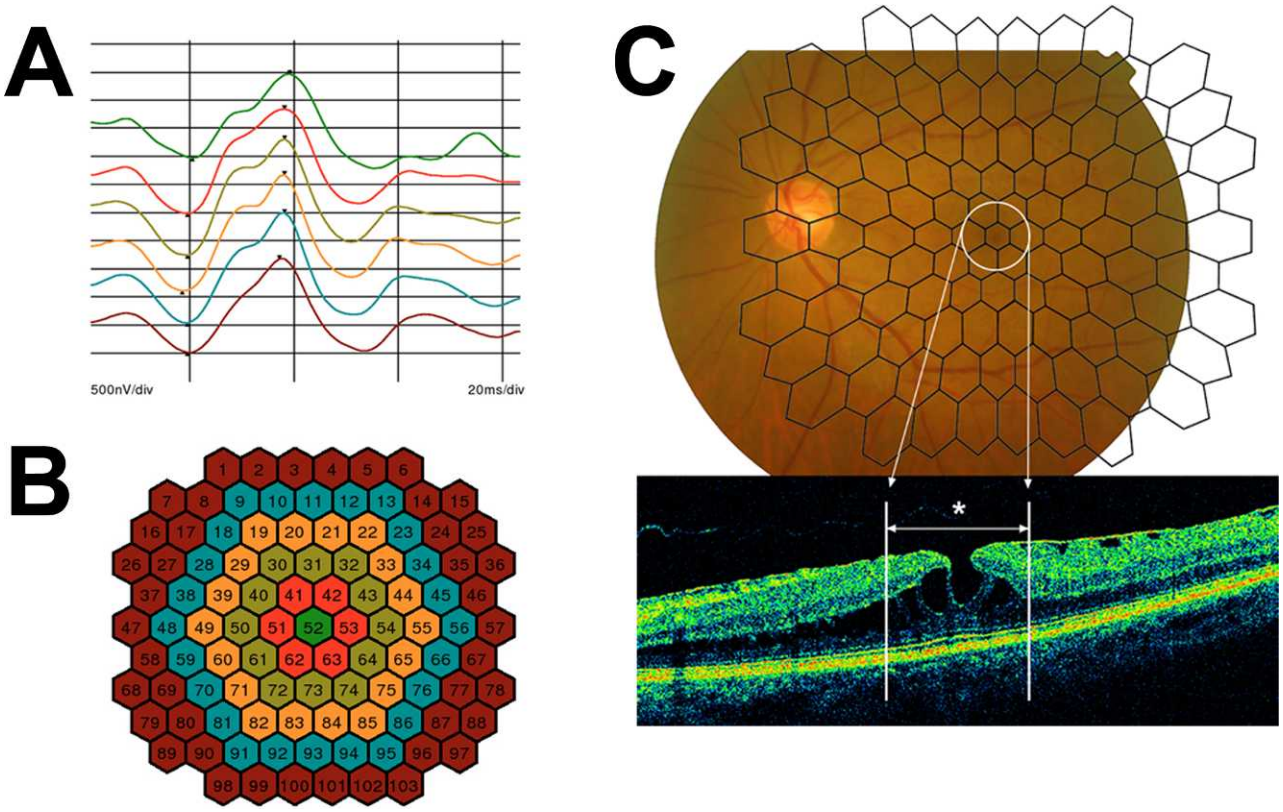

Figure 4. Images of mfERG. (**A**) Time-dependent changes in mfERG response densities in six concentric rings. (**B**) The 103 hexagonal elements that compose the six concentric rings. (**C**) The 103 hexagonal elements projected onto the corresponding retinal area. The foveal area depicted in Figure 1 (1.5-mm diameter) covers the whole central ring (R1) and a portion of the first paracentral ring (R2).

well as to calculate the sensitivity and specificity of these parameters. For all analyses, a value of $P < 0.05$ was considered statistically significant. All statistical analyses were performed using a commercial analytical software package (SPSS 13.0 for Windows software; SPSS, Inc., Chicago, IL). Graphic data were refined using a statistical graphics software package (SigmaPlot 10.0 for Windows software; Systat Software Inc., San Jose, CA).

Results

A total of 71 patients, ranging in age from 29 to 79 years (mean ± SD, 64.1 ± 9.8 years), met our inclusion/exclusion criteria. Table 1 shows the BCVA, mfERG, and SD-OCT results of affected and unaffected eyes in all 71 patients. BCVA was significantly lower in affected than that in unaffected eyes ($P < 0.001$). Moreover, mfERG amplitudes in R1 and R2 were significantly lower in affected than those in unaffected eyes. CST on SD-OCT was significantly higher in affected eyes than that in unaffected eyes ($P < 0.001$).

Table 2 shows the results of BCVA, mfERG amplitude parameters, and CST of SD-OCT in the five groups of patients with ERM. We found that BCVA ($P < 0.001$), mfERG P1 amplitude and density in R1, and CST in SD-OCT differed significantly among these five groups. When we assessed only patients with fovea-attached ERM (Group 1), we found that BCVA was progressively aggravated from Group 1A to Group 1C, with the difference among these three groups being statistically significant ($P = 0.001$). We also found that mfERG P1 amplitude density in R1 progressively decreased from Group 1A (104.2 nV/deg^2) to Group 1B (71.7 nV/deg^2) to Group 1C (54.4 nV/deg^2) ($P = 0.015$, ANOVA), but that this decline was not observed in R2 ($P = 0.275$). In addition, CST

Table 1. BCVA, mfERG Parameters, and CST on SD-OCT in Affected and Unaffected Eyes of Patients with Idiopathic Unilateral ERM

		Affected Eyes (SD)	Unaffected Eyes (SD)	*P**
BCVA, mean logMAR		0.33 (0.23)	0.07 (0.09)	0.000
Ring 1	P1 amplitude density (nV/deg^2)	87.9 (58.2)	131.3 (72.0)	0.000
	N1 amplitude (μV)	0.26 (0.18)	0.40 (0.35)	0.002
	P1 amplitude (μV)	0.73 (0.46)	1.08 (0.57)	0.000
Ring 2	P1 amplitude density (nV/deg^2)	80.7 (40.7)	95.3 (39.6)	0.000
	N1 amplitude (μV)	0.29 (0.17)	0.36 (0.18)	0.001
	P1 amplitude (μV)	0.91 (0.43)	1.07 (0.41)	0.001
Central subfield thickness (μm)		453.6 (101.5)	249.9 (22.5)	0.000

BCVA, best-corrected visual acuity; mfERG, multifocal electroretinogram; CST, central subfield thickness; SD-OCT, spectral-domain optical coherence tomography; ERM, epiretinal membrane; logMAR, logarithm of the minimal angle of resolution; SD, standard deviation.

* Paired *t*-test.

Table 2. BCVA, mfERG Amplitude Parameters, and CST on SD-OCT of Eyes with the Five Morphologic Subtypes of Idiopathic ERM

		Group 1A (SD)	Group 1B (SD)	Group 1C (SD)	Group 2A (SD)	Group 2B (SD)	P*	Tukey Post Hoc Test‡
Subjects (total $n = 71$)		23	14	15	4	15	—	
Age		64.3 (11.1)	63.0 (6.2)	63.4 (13.1)	69.3 (4.8)	64.3 (8.0)	0.857	
BCVA logMAR		0.24 (0.22)	0.43 (0.16)	0.51 (0.27)	0.28 (0.09)	0.22 (0.16)	0.000†	Group 1A–1B, $P = 0.033$ Group 1A–1C, $P = 0.001$
Ring 1	N1 amplitude (μV)	0.28 (0.17)	0.28 (0.20)	0.21 (0.14)	0.29 (0.20)	0.28 (0.22)	0.747	
	P1 amplitude (μV)	0.87 (0.39)	0.62 (0.39)	0.44 (0.44)	0.90 (0.75)	0.88 (0.45)	0.023†	Group 1A–1C, $P = 0.008$
	P1 amplitude density (nV/deg^2)	104.2 (50.1)	71.7 (48.9)	54.4 (55.5)	111.3 (94.8)	107.0 (56.2)	0.032†	Group 1A–1C, $P = 0.014$
Ring 2	N1 amplitude (μV)	0.34 (0.22)	0.24 (0.14)	0.28 (0.16)	0.31 (0.11)	0.27 (0.11)	0.505	
	P1 amplitude (μV)	1.00 (0.54)	0.80 (0.36)	0.78 (0.41)	0.95 (0.11)	0.94 (0.39)	0.532	
	P1 amplitude density (nV/deg^2)	90.3 (51.9)	69.2 (32.9)	71.7 (38.4)	83.0 (8.0)	84.3 (35.7)	0.532	
Central subfield thickness (μm)		400.3(89.8)	501.4 (55.2)	556.3 (90.7)	398.3 (56.1)	402.6 (72.0)	0.000†	Group 1A–1B, $P = 0.002$ Group 1A–1C, $P = 0.000$

* By one-way ANOVA.
† $P < 0.05$.
‡ Post hoc analysis was performed in only group 1 patients. Results with $P < 0.05$ shown only in the table.

progressively increased from Group 1A (400.3 μm) to Group 1B (501.4 μm) to Group 1C (556.3 μm) ($P < 0.001$).

Table 3 shows the inter-eye ratios of Groups 1 and 2. We found that only the inter-eye ratio of P1 amplitude in R1 differed significantly among the five groups of patients. When we analyzed Group 1 alone, we found that inter-eye ratios of P1 amplitude decreased, whereas CST in SD-OCT increased, from Group 1A to Group 1B to Group 1C.

Figure 5 shows our analysis of the correlation between BCVA and P1 amplitude density in R1 and R2 with CST and IRT on SD-OCT in Group 1 patients. CST was strongly correlated with BCVA and P1 amplitude density in R1 and R2, both in fovea-attached ERMs (Group 1) and in all ERM patients. IRT was also significantly correlated with BCVA and P1 amplitude density in R1, although correlation between IRT and P1 amplitude density in R2 did not reach statistical significance ($R = -0.255$, $P = 0.068$).

Figure 6 shows the distribution of CST and IRT in patients with fovea-attached ERM (Group 1). There was minimal overlap between subgroups when IRT rather than CST was considered as a reference standard. To evaluate the predictive accuracy of IRT in distinguishing among subgroups of Group 1 patients, ROC curve analysis was performed (Fig. 7). We found that the AUROC of IRT was 0.966 ($P < 0.0001$) for distinguishing between Group 1A and Group 1B, with an optimal cutoff value of 84.03 μm, resulting in 95.7% sensitivity and 85.7% specificity. Moreover, the AUROC of IRT was 1.000 for distinguishing between Group 1B and Group 1C, with an optimal cutoff value of 146.4 μm, resulting in 100% sensitivity and 100% specificity.

Table 3. Inter-Eye Ratios of mfERG Parameters and CST on SD-OCT of Eyes with the Five Morphologic Subtypes of Idiopathic ERM

Inter-Eye Ratio (Affected Eye/Unaffected Eye)		Group 1A (SD)	Group 1B (SD)	Group 1C (SD)	Group 2A (SD)	Group 2B (SD)	P*	Tukey Post Hoc Test‡
Ring 1	N1 amplitude	1.27 (1.06)	1.23 (0.98)	0.92 (0.90)	1.52 (1.13)	1.67 (2.63)	0.743	
	P1 amplitude	0.99 (0.94)	0.72 (0.43)	0.33 (0.27)	1.40 (0.94)	1.06 (0.85)	0.021†	Group 1A–1C, $P = 0.014$
	P1 amplitude density	0.99 (0.94)	0.72 (0.43)	0.33 (0.27)	1.40 (0.94)	1.06 (0.85)	0.022†	Group 1A–1C, $P = 0.015$
Ring 2	N1 amplitude	0.90 (0.47)	0.82 (0.48)	0.87 (0.51)	1.44 (1.39)	0.83 (0.41)	0.355	
	P1 amplitude	0.91 (0.36)	0.89 (0.36)	0.67 (0.27)	1.08 (0.39)	1.00 (0.38)	0.076	
	P1 amplitude density	0.91 (0.36)	0.89 (0.37)	0.67 (0.27)	1.08 (0.39)	1.00 (0.38)	0.078	
Central subfield thickness		1.60 (0.34)	1.99 (0.21)	2.32 (0.40)	1.48 (0.29)	1.61 (0.26)	0.000†	Group 1A–1B, $P = 0.003$ Group 1A–1C, $P = 0.000$ Group 1B–1C, $P = 0.025$

* By one-way ANOVA.
† $P < 0.05$.
‡ Post hoc analysis was performed in only group 1 patients. Results with $P < 0.05$ shown only in the table.

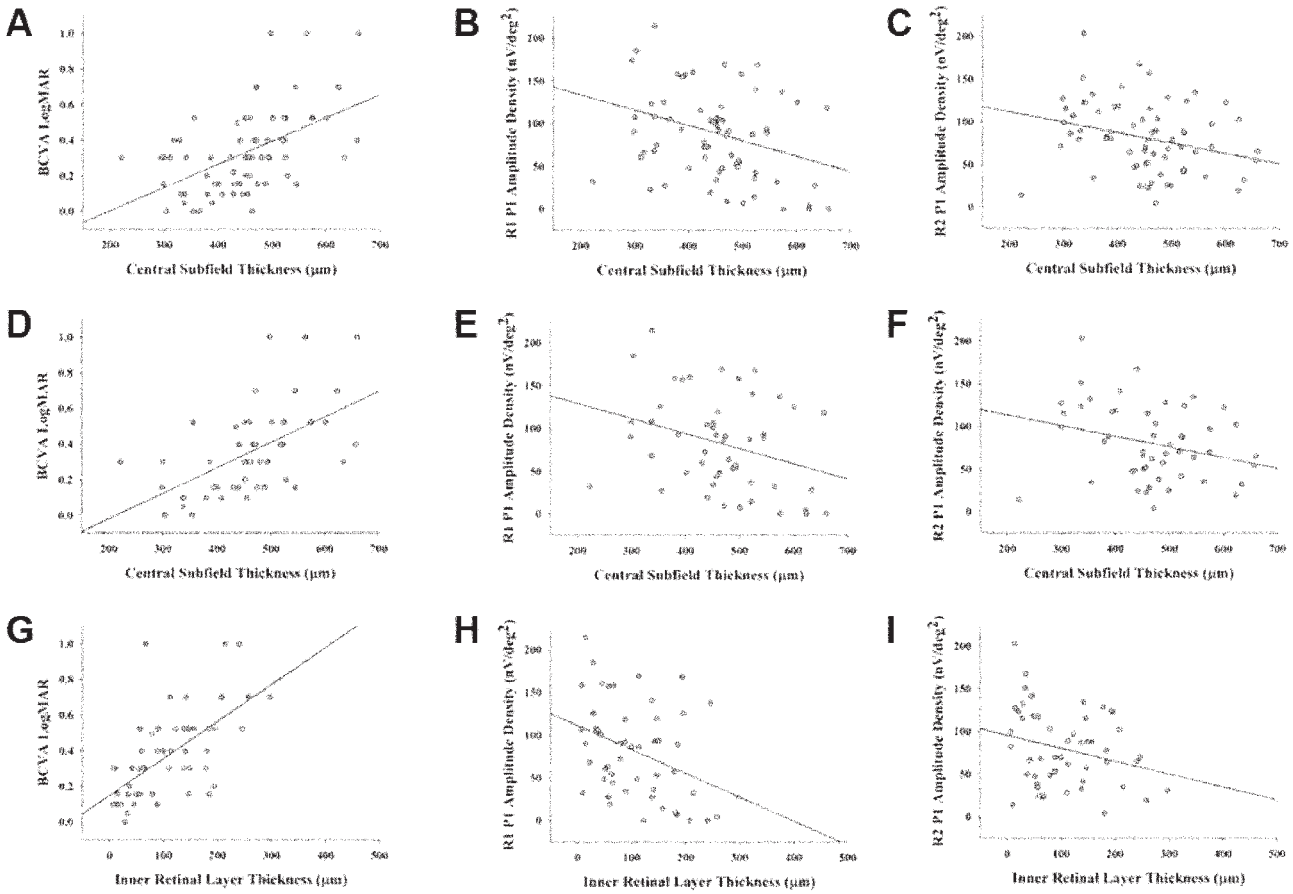

Figure 5. Correlation of BCVA and P1 amplitude density in rings 1 (R1) and 2 (R2) with CST and IRT on SD-OCT. (**A–C**) Correlations in all included ERM patients (Groups 1 and 2) between (**A**) BCVA and CST ($R = 0.567$, $P < 0.001$); (**B**) P1 amplitude density in R1 and CST ($R = -0.315$, $P = 0.007$); (**C**) P1 amplitude density in R2 and CST ($R = -0.303$, $P = 0.010$). (**D–I**) Correlations in patients with fovea-attached ERM (Group 1) between (**D**) BCVA and CST ($R = 0.605$, $P < 0.001$); (**E**) P1 amplitude density in R1 and CST ($R = -0.339$, $P = 0.014$); (**F**) P1 amplitude density in R2 and CST ($R = -0.300$, $P = 0.031$); (**G**) BCVA and IRT ($R = 0.618$, $P < 0.001$); (**H**) P1 amplitude density in R1 and IRT ($R = -0.378$, $P = 0.006$); (**I**) P1 amplitude density in R2 and IRT ($R = -0.255$, $P = 0.068$).

Discussion

Despite numerous investigations of natural history,[13] cellular pathogenesis,[14] classification,[5–7] and surgical outcomes[3] of ERM, understanding of this macular condition remains limited. ERM has been classified based on a clinical scale[5] or on OCT findings.[6,7] Recently, the degree of metamorphopsia was reported to correlate with inner nuclear layer thickness, suggesting that this parameter could be used to classify this macular condition.[15] To date, however, the objective foveal function in OCT-based morphologic subtypes of ERM had not been determined. Despite some unavoidable

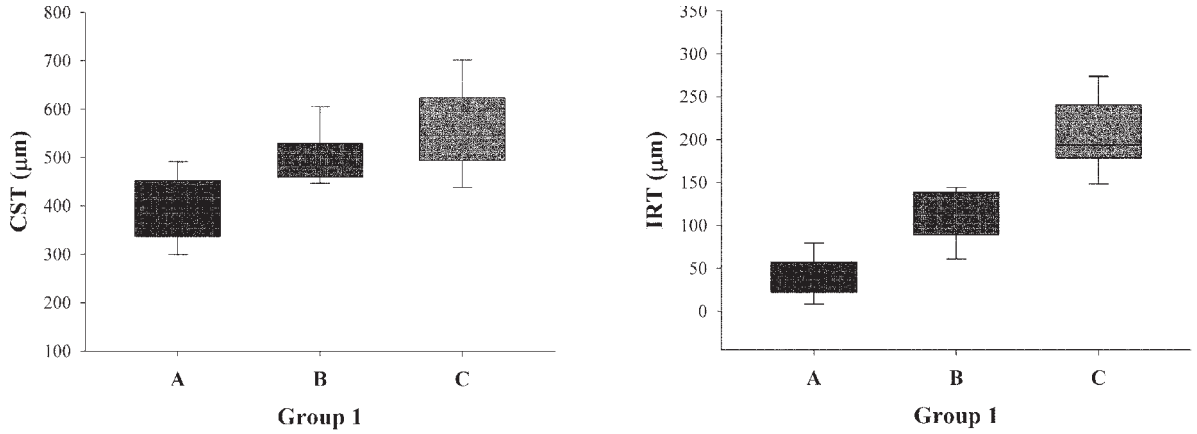

Figure 6. Distribution of CST and IRT in patients with fovea-attached epiretinal membranes (Group 1). Minimal overlap between subgroups was observed when IRT rather than CST was considered a guideline parameter for differentiation.

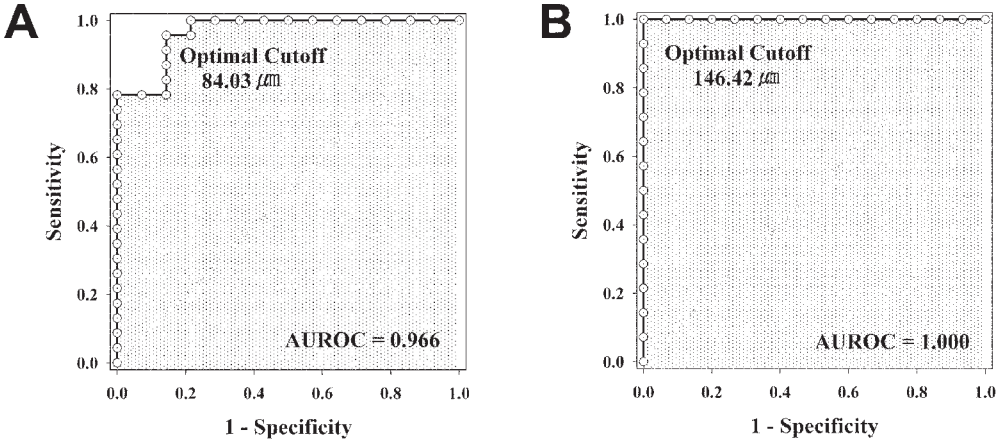

Figure 7. ROC curves of IRT in Group 1 patients. (**A**) ROC curve of IRT distinguishing Group 1B from Group 1A. AUROC curve 0.966, 95% confidence interval 0.915–1.017, $P < 0.0001$; (**B**) ROC curve of IRT distinguishing Group 1C from Group 1B. Area under the ROC curve 1.000.

subjectivity, our findings provide a basis for the morphologic grouping of ERMs.

We found that fovea-attached ERM showing outer retinal thickening with a minimal change of the inner retina generated a near-normal mfERG response (inter-eye ratio, 0.99), whereas fovea-attached ERM showing prominent inner retinal thickening on SD-OCT generated a much lower response on mfERG. We also found that thickening of the inner retinal layer at fovea was strongly correlated with decreased mfERG responses in fovea-attached ERM (Fig. 6). These findings suggest that IRT can be used as a parameter indicating the functional compromise of foveal area in the fovea-attached ERM.

We found that pseudohole-type ERM showed relatively well-preserved foveal function. This was not surprising, because this type of ERM does not cover the foveal area and has minimal influence on the electrophysiologic response of the foveal area, especially in the R1 of the mfERG average map. Interestingly, eyes with pseudohole-type ERM accompanied by schisislike intraretinal splitting (Group 2B, $n = 15$) showed near-normal mfERG responses, despite their parafoveal configuration on SD-OCT being severely distorted by the lifting force originating from fovea-sparing ERM. The amplitudes on mfERG were not decreased compared with the unaffected eye, with inter-eye response ratios of 1.06 and 1.00 for R1 and R2, respectively. These findings suggest that surgical intervention is not urgently required in patients with this type of ERM because of their well-preserved central foveal function. We suppose this schisislike intraretinal splitting is not true separation between retinal layers, but instead a form of retinal edema from traction. However, because this study did not include a longitudinal analysis, further studies with longitudinal data are needed to clarify the adverse effect of this type of ERM.

Cataracts have been shown to significantly reduce mfERG responses in the central 4–14° visual field.[16,17] Moreover, reported pseudophakic eyes with intraocular lenses showed decreased mfERG responses compared with age-matched healthy controls, suggesting that intraocular lenses have optical effects on mfERG responses.[18] This is the main limitation of studies[9,19,20] comparing pre- and postoperative mfERG responses in patients with certain retinal pathologies, since many patients who undergo vitreoretinal surgery undergo cataract surgery at the same time. To eliminate the confounding effects of cataracts and intraocular lenses on mfERG responses, we excluded all patients with intraocular lenses, visually significant cataracts, and different inter-eye cataract severity.

The pathogenesis of ERMs may differ depending on their clinical setting. Primary idiopathic ERMs may be unassociated with other ocular disorders, whereas secondary ERMs are associated with several other ocular disorders, including retinal vein occlusion, diabetic retinopathy, peripheral retinal tear, and uveitis. ERMs of differing pathogenesis may have different characteristics. Among the features that may vary are etiology, morphology, prognosis, and treatment response. ERMs can be divided into two distinct groups based on their morphologic characteristics: those with focal points of attachment to the retina and those with global adherence to the retina.[6] Idiopathic ERMs were found to be significantly less likely to have focal points of adhesion to the retina than secondary ERMs.[7] For example, 80% of idiopathic ERMs showed global adhesion patterns, whereas 52% of secondary ERMs showed partial adhesion patterns, on time-domain OCT configuration.[7] We sought to correlate CST on SD-OCT topography, which represents the average retinal thickness in the central 1-mm area, with mfERG parameters, by investigating a representative SD-OCT raster scan image. Because the representativeness of these images may be weak in ERMs with focal adhesion patterns, a characteristic more frequent in secondary ERMs, we attempted to minimize this bias by including only idiopathic ERMs, which demonstrate diffuse thickening of macula by global adhesion. Moreover, since secondary causes of ERM may affect visual acuity and electrophysiologic responses, independent of ERM effects, we excluded patients with secondary ERMs from correlation analyses among BCVA, SD-OCT, and mfERG parameters. Although previous studies[21,22] did not show significant correlations between CST and BCVA in patients with idiopathic ERM, we found that CST in SD-OCT was significantly correlated with BCVA and P1 amplitude in R1 and R2. When fovea-sparing ERMs were excluded, the strength of these correlations for CST increased for BCVA ($R = 0.605$) and for P1 amplitude density in R1 ($R = -0.339$) and R2 ($R = 0.300$). The correlations were greater for IRT with BCVA ($R = 0.618$) and P1 amplitude density in R1 ($R = -0.378$). Since we calculated IRT in the center of the foveal area on the representative scan image, the correlation between IRT and P1 amplitude density in R2 was not significant ($R = -0.255$, $P = 0.068$). These results suggest that at least in fovea-attached ERMs, CST and IRT in SD-OCT can be used to evaluate the functional compromise of the foveal area.

This study had several limitations. First, we enrolled only patients scheduled for surgical intervention; therefore, subclinical ERM patients were not included. We also did not include patients with secondary ERM caused by other

vitreoretinal pathologies (e.g., diabetic retinopathy, retinal vein occlusion, uveitis, retinal tear). Thus, our results may not be representative of findings in all possible morphologic subtypes of ERM, and cannot be extrapolated to patients with either subclinical or secondary ERM. Second, the classification system we used for primary idiopathic ERM was based on our subjective interpretation of representative SD-OCT scan images, although we showed the relevance of this classification by ROC curve analysis of CST and IRT.

In conclusion, the present findings suggest that mfERG can be used to assess the pathophysiology of ERM and to evaluate the degree of functional demise in the foveal area on SD-OCT. These findings may provide additional information in choosing the optimal timing of surgical intervention in patients with ERM.

References

1. Massin P, Allouch C, Haouchine B, et al. Optical coherence tomography of idiopathic macular epiretinal membranes before and after surgery. *Am J Ophthalmol*. 2000;130:732–739.
2. Margherio RR, Cox MS Jr, Trese MT, Murphy PL, Johnson J, Minor LA. Removal of epimacular membranes. *Ophthalmology*. 1985;92:1075–1083.
3. McDonald HR, Verre WP, Aaberg TM. Surgical management of idiopathic epiretinal membranes. *Ophthalmology*. 1986;93:978–983.
4. Wong JG, Sachdev N, Beaumont PE, Chang AA. Visual outcomes following vitrectomy and peeling of epiretinal membrane. *Clin Exp Ophthalmol*. 2005;33:373–378.
5. Gass JDM. *Stereoscopic Atlas of Macular Diseases: Diagnosis and Treatment*. 3rd ed. St. Louis: Mosby; 1987.
6. Wilkins JR, Puliafito CA, Hee MR, et al. Characterization of epiretinal membranes using optical coherence tomography. *Ophthalmology*. 1996;103:2142–2151.
7. Mori K, Gehlbach PL, Sano A, Deguchi T, Yoneya S. Comparison of epiretinal membranes of differing pathogenesis using optical coherence tomography. *Retina*. 2004;24:57–62.
8. Sutter EE, Tran D. The field topography of ERG components in man—I. The photopic luminance response. *Vision Res*. 1992;32:433–446.
9. Moschos M, Apostolopoulos M, Ladas J, et al. Assessment of macular function by multifocal electroretinogram before and after epimacular membrane surgery. *Retina*. 2001;21:590–595.
10. Lim JW, Cho JH, Kim HK. Assessment of macular function by multifocal electroretinography following epiretinal membrane surgery with internal limiting membrane peeling. *Clin Ophthalmol*. 2010;4:689–694.
11. Early Treatment Diabetic Retinopathy Study design and baseline patient characteristics. ETDRS report number 7. *Ophthalmology*. 1991;98:741–756.
12. Hood DC, Bach M, Brigell M, et al. ISCEV guidelines for clinical multifocal electroretinography (2007 edition). *Doc Ophthalmol*. 2008;116:1–11.
13. Fraser-Bell S, Guzowski M, Rochtchina E, Wang JJ, Mitchell P. Five-year cumulative incidence and progression of epiretinal membranes: the Blue Mountains Eye Study. *Ophthalmology*. 2003;110:34–40.
14. Hirokawa H, Jalkh AE, Takahashi M, Trempe CL, Schepens CL. Role of the vitreous in idiopathic preretinal macular fibrosis. *Am J Ophthalmol*. 1986;101:166–169.
15. Watanabe A, Arimoto S, Nishi O. Correlation between metamorphopsia and epiretinal membrane optical coherence tomography findings. *Ophthalmology*. 2009;116:1788–1793.
16. Tam WK, Chan H, Brown B, Yap M. Effects of different degrees of cataract on the multifocal electroretinogram. *Eye*. 2004;18:691–696.
17. Wordehoff UV, Palmowski AM, Heinemann-Vernaleken B, Allgayer R, Ruprecht KW. Influence of cataract on the multifocal ERG recording—a pre- and postoperative comparison. *Doc Ophthalmol*. 2004;108:67–75.
18. Palmowski-Wolfe AM, Woerdehoff U. A comparison of the fast stimulation multifocal-ERG in patients with an IOL and control groups of different age. *Doc Ophthalmol*. 2005;111:87–93.
19. Si YJ, Kishi S, Aoyagi K. Assessment of macular function by multifocal electroretinogram before and after macular hole surgery. *Br J Ophthalmol*. 1999;83:420–424.
20. Ma J, Yao K, Jiang J, et al. Assessment of macular function by multifocal electroretinogram in diabetic macular edema before and after vitrectomy. *Doc Ophthalmol*. 2004;109:131–137.
21. Inoue M, Morita S, Watanabe Y, et al. Preoperative inner segment/outer segment junction in spectral-domain optical coherence tomography as a prognostic factor in epiretinal membrane surgery. *Retina*. 2011;31:1366–1372.
22. Falkner-Radler CI, Glittenberg C, Hagen S, Benesch T, Binder S. Spectral-domain optical coherence tomography for monitoring epiretinal membrane surgery. *Ophthalmology*. 2010;117:798–805.